A kinetic assessment of the *C. elegans* amyloid disaggregation activity enables uncoupling of disassembly and proteolysis

Jan Bieschke,[1†] Ehud Cohen,[2†] Amber Murray,[1] Andrew Dillin,[2] and Jeffery W. Kelly[1*]

[1]Departments of Chemistry and Molecular and Experimental Medicine, The Skaggs Institute for Chemical Biology, The Scripps Research Institute, La Jolla, California 92037

[2]The Howard Hughes Medical Institute and Molecular and Cell Biology Laboratory, The Salk Institute for Biological Studies, La Jolla, California 92037

Received 27 May 2009; Accepted 13 August 2009
DOI: 10.1002/pro.234
Published online 21 August 2009 proteinscience.org

Abstract: Protein aggregation is a common feature of late onset neurodegenerative disorders, including Alzheimer's disease. In Alzheimer's disease, misassembly of the Aβ peptide is genetically linked to proteotoxicity associated with disease etiology. A reduction in Aβ proteotoxicity is accomplished, in part, by the previously reported Aβ disaggregation and proteolysis activities–under partial control of heat shock factor 1, a transcription factor regulating proteostasis in the cytosol and negatively regulated by insulin growth factor signaling. Herein, we report an improved *in vitro* assay to quantify recombinant fibrillar Aβ disaggregation kinetics accomplished by the exogenous application of *C. elegans* extracts. With this assay we demonstrate that the Aβ disaggregation and proteolysis activities of *C. elegans* are separable. The disaggregation activity found in *C. elegans* preparations is more heat resistant than the proteolytic activity. Aβ disaggregation in the absence of proteolysis was found to be a reversible process. Future discovery of the molecular basis of the disaggregation and proteolysis activities offers the promise of delaying the age-onset proteotoxicity that leads to neurodegeneration in a spectrum of maladies.

Keywords: disaggregation; proteolysis; abeta; Alzheimer's disease

Introduction

Protein aggregation is genetically and biochemically linked to the development of human neurodegenerative disorders, such as Alzheimer's disease (AD), Parkinson's disease (PD), Huntington's disease (HD), the familial amyloidoses, and the prion disorders.[1–7] Aggregation of the 40- and 42-amino-acid amyloid beta peptides ($A\beta_{40}$ and $A\beta_{42}$) putatively causes AD.[8] Whether Aβ proteotoxicity arises from within the neuron, outside the cell, or both, how toxicity is effected and what the structure(s) of the cytotoxic agent is, are key unanswered questions. A prominent risk factor common to all of these neurodegenerative diseases is aging.[9–14] Insulin/Insulin growth factor-1 signaling (IIS) is perhaps the most prominent signaling pathway

Additional Supporting Information can be found in the online version of this article.

[†]Jan Bieschke and Ehud Cohen contributed equally to this work.

Jan Bieschke's current address is Max-Delbrück-Center for Molecular Medicine, Robert-Roessle-Str. 10, Berlin-Buch 13125, Germany.

Ehud Cohen's current address is Institute of Medical Research Israel Canada (IMRIC), The Hebrew University of Jerusalem, Ein-Karem, Jerusalem 91121, Israel.

Grant sponsor: NGFNplus; Grant number: 01GS08132; Grant sponsor: NIH; Grant number: AG031097; Grant sponsors: The Bundy Foundation, the Helmholz Gemeinschaft, the Skaggs Institute for Chemical Biology, and the Lita Annenberg Hazen Foundation.

*Correspondence to: Jeffery W. Kelly, The Scripps Research Institute, BCC 265, 10550 N. Torrey Pines Road, La Jolla, CA 92037. E-mail: jkelly@scripps.edu

regulating aging. Reduced IIS is linked to longevity in worms,[15] flies, mice,[16] and humans.[17,18] In worms, lifespan extension facilitated by IIS reduction (either by mutating the sole insulin/IGF receptor, *daf-2,* or by the application of RNAi directed against *daf-2*) is dependent upon the activities of the transcription factors DAF-16 and HSF-1.[19,20]

Why aging is the prominent risk factor in human neurodegenerative diseases is not completely understood. Some insight regarding the connection between aging and neurodegeneration is provided by recent studies demonstrating that delaying aging in organismal models of HD and AD by IIS suppression ameliorates aggregation-associated proteotoxicity.[9,12,19,21,22] The molecular basis for the link between the reduction in IIS and diminished proteotoxicity is likely because aging signaling pathways and their transcriptomes have a strong influence on the protein homeostasis (or proteostasis) network, that is, the biological pathways that maintain our proteome and minimize aggregate accumulation.[9] For example, both the heat shock response controlling proteostasis in the cytosol, and longevity mediated by reduced IIS require the transcription factor, HSF-1. As is the case for lifespan extension, both the DAF-16 and HSF-1 transcriptomes are required to ameliorate $A\beta_{42}$ proteotoxicity via IIS suppression.[22]

Speculation[23] that a specialized mammalian disaggregation activity, possibly involving chaperones, enables aggregate degradation has some experimental support.[22,24] Active and passive immunization studies resulting in the clearance of Aβ deposits from AD animal models suggest that inducing degradation pathways can be therapeutically beneficial.[25,26] In one potential model of the disaggregase activity, the disassembly of fibrillar Aβ aggregates is envisioned to be driven by proteolysis of Aβ monomers, which would lead to the disassembly of Aβ aggregates by depleting the monomers below their critical concentration, causing dissociation of the fibrils to repopulate the disappearing monomer population.[27,28] Alternatively, disaggregation via a specific cellular pathway or utilizing a macromolecular complex could take apart Aβ fibrils, independent of proteolysis. This scenario would enable reaggregation of Aβ into fibrils if Aβ monomer proteolysis was inhibited and the disaggregase activity was depleted. Discovering the molecular underpinnings of the *C. elegans* fibril disaggregase pathway(s)/activity(ies) and/or the degradation pathway(s)/activity(ies) could reveal novel therapeutic strategies for human neurodegenerative diseases.[9,22] In this manuscript, we focus primarily on the disaggregase activity.

The apparent importance of disaggregation and degradation in countering $A\beta_{42}$ aggregation-associated proteotoxicity and the linkage of this biological pathway(s) or activity(ies) to aging-associated signaling pathways[22] motivated us to optimize and further scrutinize the Aβ disaggregation assay to discern whether the disaggregation and proteolysis activities are separable. In this study, the Aβ amyloid fibril-thioflavin T (ThT) fluorophore complex prepared *in vitro* was treated with *C. elegans* homogenate to discern the rate of fibril disassembly and the degree of Aβ proteolysis in the presence or absence of selected protease inhibitors. We utilized the decrease in ThT fluorescence to follow disaggregation (verified by atomic force microscopy) and the decrease in immunoreactivity to Aβ antibodies and/or an HPLC assay to monitor the degradation of Aβ. These studies demonstrate that disaggregation does not require proteolytic degradation, as these activities are separable.

Results

C. elegans *homogenate possesses* $A\beta_{40}$ *fibril disaggregation activity*

To assess the disaggregation activity within the *C. elegans* AD model, we prepared cellular extracts by homogenizing worms grown on bacteria to day one of adulthood. The debris from Aβ worm homogenization was cleared by low speed centrifugation (as detailed in the Methods section) and the resulting postdebris supernatant (PDS) was used in subsequent experiments. Since the disaggregation machinery might be inducible, we used worms that express $A\beta_{42}$ in their smooth body wall muscles under control of the *unc54* promoter that encodes the myosin heavy chain gene and is expressed from embryogenesis through adulthood (strain CL 2006[21]), hereafter referred to as Aβ worms. We assumed that $A\beta_{42}$ overexpression in these worms would be sufficient to induce this activity. These Aβ worms were grown on bacteria to day one of adulthood, at which stage no proteotoxicity is observed.[21,22] Worms not expressing $A\beta_{42}$ (wild-type worms, strain N2) were used as controls. Worm PDS was added to preformed $A\beta_{40}$ (or $A\beta_{42}$) fibrils *in vitro* to assess its disaggregation activity.

Aβ fibrils were generated from monomerized Aβ, prepared from $A\beta_{40}$ (or $A\beta_{42}$) peptide dissolved in hexafluoroisopropanol (HFIP) overnight, then lyophilized, dissolved at pH 10.5, and filtered through a low molecular weight membrane filter (Microcon YM-10, Millipore) to remove covalent and noncovalent aggregates.[29] Fibrillar aggregates were then formed by incubating the initially monomeric Aβ peptide (50 μM) at 37°C at pH 7.4 for 3 days, during which time the sample was agitated using an overhead rotary shaker (20 rpm). Amyloidogenesis was monitored by ThT fluorescence (Supporting information Fig. S1A). ThT is a fluorophore that exhibits a higher fluorescence quantum yield and a red shift upon binding to fibrils or spherical aggregates.[30] Aggregates were characterized by circular dichroism spectroscopy to observe the expected increase in β-sheet structure (Supporting information Fig. S1B), and by atomic force microscopy (AFM) to confirm the fibril morphology (Supporting information

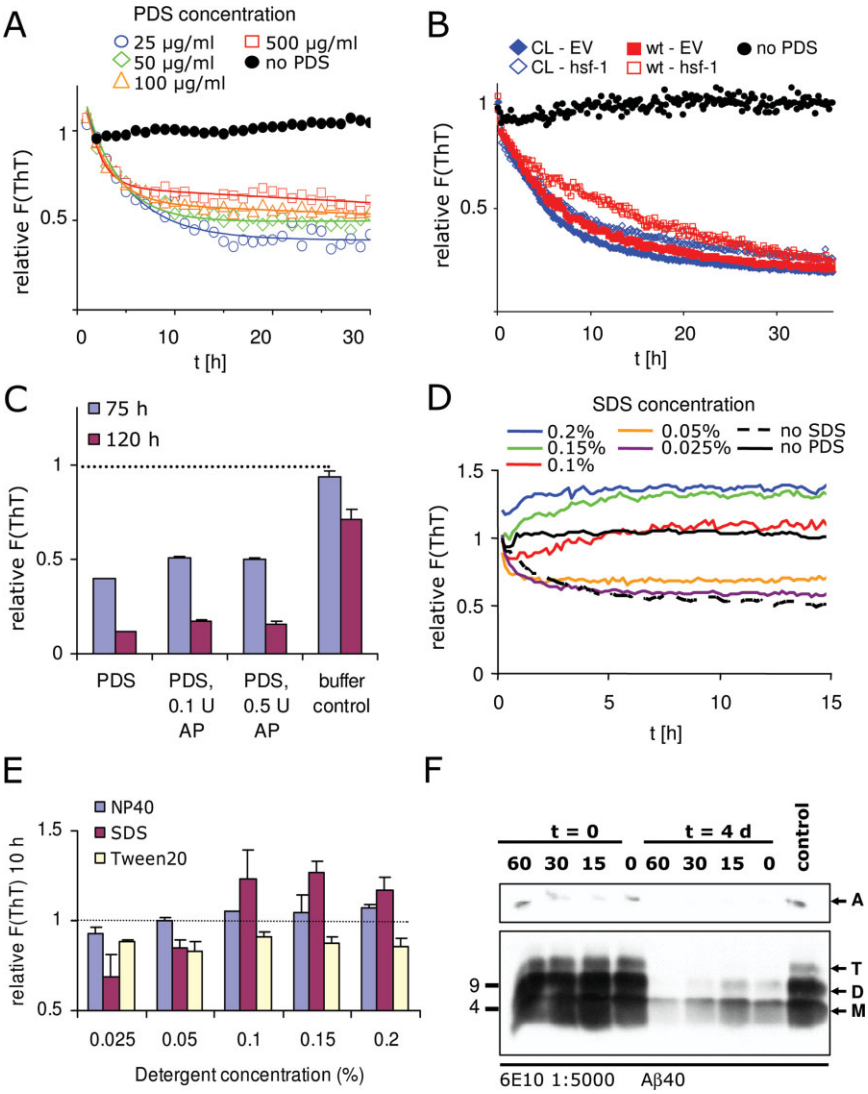

Figure 1. $A\beta_{40}$ disaggregation activity A: Disaggregation activities of *C. elegans* PDS as a function of total protein concentration (25–500 µg/mL). Lines show mono-exponential decay function fits to the data (open symbols). B: Disaggregation activities of PDS (20 µg/mL) from $A\beta_{42}$-expressing (CL for CL2006) and wt (N2) *C. elegans* fed bacteria expressing *hsf-1* RNAi or empty vector controls (EV). Neither the disaggregation rate nor its reduction by *hsf-1* downregulation depend on $A\beta_{42}$ expression. C: PDS-mediated $A\beta_{40}$ disaggregation is not discernibly inhibited when ATP in the PDS is hydrolyzed by pretreatment with apyrase (AP, 0.1 and 0.5 U, 15 min, 30°C); average relative ThT signals of quintuplicate samples ± SD. D: PDS-mediated (PDS, 25 µg/mL) $A\beta_{40}$ disaggregation kinetics in the presence of 0.025–0.2% SDS. ThT signals of detergents in buffer were subtracted from the Aβ signals. E: Relative ThT fluorescence signals after 10 h incubation with PDS in the presence of 0.025–0.2% SDS, Tween-20, or NP-40. F: Separation of PDS-mediated disaggregation and proteolysis products of $A\beta_{40}$ by denaturing PAGE visualized by Western blot analysis (mAb 6E10) of fibrillar $A\beta_{40}$ before and after PDS treatment. Aβ samples were sonicated for 0, 15, 30, or 60 min before disaggregation. Arrows indicate apparent monomer (M), dimer (D), and trimer (T) bands as well as high-MW aggregate (A) bands. Control: fibrillar $A\beta_{40}$ incubated for 4 d in the absence of PDS.

Fig. S1C). Fibrillar aggregates were sonicated for 30 min using a water bath sonicator to afford a uniform (200–500 nm) length distribution of fibrils (Supporting information Fig. S1D). Disaggregation of the presonicated fibrils was monitored in a fluorescence plate reader by the decrease in ThT fluorescence over time, with data being collected every 10 min following 5 s of shaking.[31] Disaggregation of Aβ fibrils was confirmed by AFM.[22]

The ability of worm PDS to disaggregate $A\beta_{40}$ fibrils in phosphate buffer (150 m*M* NaCl, 50 m*M* Na-phosphate, pH 7.4) at 37°C was scrutinized by the addition of Aβ worm PDS at final total PDS protein concentrations ranging from 25 to 500 µg/mL [Fig. 1(A)]. ThT (20 µM) fluorescence decreased in the presence of worm PDS, whereas incubation with buffer alone (black circles) did not significantly change the ThT fluorescence. Disaggregation time courses for all PDS reactions were fitted by mono-exponential decay functions [Fig. 1(A), lines]. Disaggregation time constants were 4.6 ± 0.6, 3.4 ± 0.3, 2.5 ± 0.2, and 1.5 ± 0.1 h for PDS exhibiting a total protein concentration of 25, 50, 100,

and 500 μg/mL, respectively. While increasing PDS concentrations accelerated disaggregation as expected, increasing PDS concentrations also increased residual ThT fluorescence, either as a consequence of fluorescence induced by ThT binding to worm protein(s) or as a result of competing activities in the PDS, such as proteolysis which could disable the disaggregase activity.

Next, we compared the disaggregation activities of Aβ worms to those of wt control (N2) worms to determine whether the *C. elegans* disaggregation activity or its inhibition by *hsf-1* downregulation depends on the expression of the Aβ peptide. PDS (25 μg/mL total protein) prepared from $A\beta_{42}$-expressing (CL2006) worms or N2(wt) worms grown on *hsf-1* RNAi or on noncoding (EV) RNAi was added to presonicated fibrillar $A\beta_{40}$ and Aβ disaggregation was monitored by ThT fluorescence for 36 h [Fig. 1(B)]. Downregulation of *hsf-1* expression resulted in a reduced disaggregation activity in both wt and Aβ worms (cf. open and closed symbols). Though small differences between the disaggregase activities could be observed in both worm strains, it is clear that the disaggregase activity is constitutive. That said, Aβ expression could lead to more HSF-1 activity and slightly enhanced activity.

We then proceeded to further characterize the disaggregation activity by exploring the influence of NaCl concentration and the length of time the Aβ fibrils were sonicated before being treated with Aβ worm PDS. NaCl concentration had little influence on the disaggregase activity (Supporting information Fig. S2A), whereas prolonged presonication of Aβ fibrils hastened disaggregation (Supporting information Fig. S2B). While sonication is not required to achieve disaggregation (Supporting information Fig. S2B), the number of accessible fibril ends is a significant factor in determining the disaggregation rates. On the other hand, NaCl, which is known to promote fibril formation and would be expected to electrostatically stabilize Aβ amyloid fibrils,[32] does not have a measurable influence.

Disaggregation could be an ATP driven process. To test this hypothesis, we preincubated Aβ worm PDS with apyrase (0.1 and 0.5 U) for 15 min at 30°C before adding the treated PDS to $A\beta_{40}$ fibrils (15 μM_{monomer}) in PBS. Under these conditions, we have demonstrated that the accessible ATP is hydrolyzed (see Methods). No dependence of the disaggregation activity on apyrase concentration was observed, as ascertained by monitoring ThT fluorescence intensity at 75 h (50% complete) and 120 h (80% complete) into the disaggregation time course, [Fig. 1(C)]. Likewise, no dependence of the disaggregation activity on ATP was observed in the presence of protease inhibitor cocktail or upon addition of the competitive inhibitor ATP-γ-S. However, these experiments do not definitively exclude a requirement for ATP, as vesicular ATP could drive the process. Additional experiments are ongoing to further scrutinize the ATP dependence of the disaggregase activity.

Worm PDS was subjected to centrifugation to separate the soluble and membrane components. We found that the majority of the disaggregation activity could be pelleted at 100,000 × g (Supporting information Fig. S2C), suggesting that the disaggregation activity can associate with membranes. We therefore assessed the impact of the nonionic detergents NP-40 and Tween-20, and the ionic detergent SDS [Fig. 1(D,E)] on the disaggregation activity of PDS at detergent concentrations ranging from 0.025 to 0.2%. The detergents SDS and NP-40 largely eliminate disaggregation activity at concentrations ≥0.1% (w/v), whereas Tween-20 induced a moderate reduction in disaggregation activity over the whole concentration range [Fig. 1(E)]. No clear correlation of the detergents' effects with their respective critical micelle concentrations could be inferred.

SDS accelerated disaggregation at concentrations below 0.1%, suggesting that SDS may weaken Aβ fibril structures by partial denaturation and thus promote disaggregation. Independent of the disaggregation activity, SDS concentrations ≥ 0.1% led to a gradual increase in the Aβ fibril fluorescence signal [Fig. 1(D,E)], suggesting that SDS may promote the accessibility of Aβ fibrils for the ThT dye. Background fluorescence signals resulting from ThT binding to detergent micelles were subtracted from all ThT kinetic measurements. Detergent-only ThT fluorescence remained constant over the course of the experiment (Fig S3).

The ability of the detergents to inhibit the disaggregase activity at higher concentrations is compatible with several interpretations, including the hypothesis that the disaggregation activity is membrane associated and/or that the disaggregase has a quaternary structure that is detergent sensitive. It is also possible that detergents disrupt the interaction between the disaggregation machinery and the Aβ fibrils. How the detergents influence the disaggregation activity is an area of ongoing investigation.

The disaggregated Aβ peptide is proteolyzed by worm PDS

To quantify the $A\beta_{40}$ concentration before and after disaggregation by PDS, $A\beta_{40}$ fibrils were sonicated for 0, 15, 30, or 60 min and then subjected to disaggregation by PDS [Fig. 1(F)]. SDS soluble and insoluble $A\beta_{40}$ was quantified by Western blot analysis using two separate monoclonal Aβ antibodies (clones 6E10 and 4G8) to visualize Aβ before ($t = 0$) and after being subjected to worm PDS for 4 days [Fig. 1(F), 6E10 data shown, see Supporting information Fig. S2D for 4G8 data]. The amounts of monomeric (M), apparent dimeric (D), and apparent trimeric (T) forms of SDS soluble $A\beta_{40}$ were dramatically decreased after treating the $A\beta_{40}$ fibrils with PDS for 4 days, implying that after disaggregation, $A\beta_{40}$ peptides were proteolyzed by components of the worm PDS. Prolonged sonication did not affect the amount of $A\beta_{40}$ detected before

disaggregation, but reduced the residual monomer, dimer, and trimer bands observed after treatment with PDS, consistent with more complete disaggregation and proteolysis when starting with smaller fibrils [Fig. 1(F), Supporting information Fig. S2B]. Note the steeper decline in the ThT signal of $A\beta_{40}$ fibrils subjected to prolonged sonication before treating them with PDS (Supporting information Fig. S2B).

The C. elegans *disaggregation activity is separable from the proteolytic activity*

As mentioned earlier, different models could explain the PDS-mediated $A\beta_{40}$ disaggregation and proteolysis activity observed. First, proteolysis of monomers could drive disaggregation by lowering the monomer concentration below the critical concentration for Aβ fibril formation.[28] A second possibility is that direct proteolytic digestion of fibrillar Aβ could also result in disaggregation. Since these models require proteolysis for disaggregation, inhibiting proteolysis should preclude disaggregation if these models apply. An alternative model recognizes that disaggregation and proteolysis could be separable activities and allows for disaggregation in the absence of proteolysis. Both activities could either be mediated by different components or pathways of the *C. elegans* proteome or by the same component(s) or pathway(s), having distinct active sites.[33]

To distinguish between these two mechanistic categories, we tested whether disaggregation and proteolysis could be uncoupled utilizing protease inhibitors. Fibrillar aggregates of either synthetic $A\beta_{42}$ or $A\beta_{40}$ peptides were treated with worm PDS in the absence or presence of protease inhibitors. Sodium azide (0.02%) was added to preclude potential proteolytic activity caused by bacterial growth during disaggregation time courses of up to 75 h. Both $A\beta_{40}$ and $A\beta_{42}$ fibrillar aggregates are readily detected by AFM in ThT-positive samples before, but not after incubation with PDS, either in the presence or absence of Roche complete protease inhibitor cocktail (PIC) [Fig. 2(A) and Ref. 22] demonstrating disaggregation. Very similar ThT-monitored disaggregation time courses were observed in the absence and presence of PIC for $A\beta_{42}$ fibrils [Fig. 2(B)], as well as for the first 24 h of $A\beta_{40}$ disaggregation reaction [Fig. 4(A)], suggesting that proteolysis is not required for disaggregation.

To test whether the addition of PIC prevented proteolysis of $A\beta_{40}$ and $A\beta_{42}$ after PDS-mediated disaggregation for 72 h, the Aβ aggregates and monomers were denatured and resolved by SDS-PAGE after PDS treatment. Nearly complete proteolysis was observed in PDS samples lacking PIC, whereas monomeric $A\beta_{40}$ [Fig. 2(C)] or an equilibrium mixture of monomeric (M) and tetrameric (T) $A\beta_{42}$ structures as well as SDS-soluble aggregates (A_{sol}) [Fig. 2(D)] was observed in the presence of PIC. Collectively, these experiments demonstrate that disaggregation can occur upon inhibition of proteolysis.

To more accurately quantify the different $A\beta_{40}$ species, especially aggregates, and to avoid possible under-representation of SDS-insoluble $A\beta_{40}$ that might not enter the gel or that might fail to be transferred, we used membrane-based filter retardation assays and dot blots as complementary assays. Dot blots without added SDS were used to quantify total $A\beta_{40}$, including monomeric, oligomeric, and aggregated species. In parallel, Aβ samples were denatured by boiling in 2% SDS and filtered through a cellulose acetate membrane (0.2 μm), where only large SDS-insoluble Aβ aggregates are retained on the membrane [Fig. 2(E)].[5] $A\beta_{40}$ retained on the membrane was detected using the 6E10 antibody and quantified from triplicate samples. Our results indicate that disaggregation by worm PDS reduced SDS-insoluble $A\beta_{40}$ aggregates by 70–80% [Fig. 2(E,F)]. However, proteolysis of $A\beta_{40}$ was largely prevented by the addition of PIC or phenylmethylsulphonyl fluoride (PMSF) [Fig. 2(E,F)]. Fig. 2(E) also demonstrates that heat inactivation of the PDS-associated disaggregase activity (95°C, 10 min) prevents disaggregation and proteolysis, as reported previously.[22]

The disaggregation activity is more temperature resistant than the protease activity

To evaluate the sensitivity of the disaggregation activity to thermal denaturation, we incubated PDS at 37, 70, 80, or 95°C for 10 min before its addition to fibrillar $A\beta_{40}$. Only a moderate decline in disaggregation activity is observed upon treatment at 70 or 80°C [Fig. 3(A), cf. blue and green lines to black line], whereas heating to 95°C substantially diminished disaggregation activity (orange line).

The relative amounts of total and SDS-resistant $A\beta_{40}$ aggregates [Fig. 3(B,C), respectively] were quantified by dot blot and filter retardation assays and normalized to the untreated fibrillar Aβ control. Heat treatment at 80°C inactivated proteolysis [Fig. 3(B)] but not the disaggregation activity, as evidenced by the fact that the amount of SDS-resistant aggregates were significantly reduced [Fig. 3(C)] when compared with PDS heat treated at 95°C. Analogous results were independently obtained for $A\beta_{42}$ [Fig. 3(D)] by quantifying the soluble (M, T) and aggregate (A) bands from $A\beta_{42}$ Western blots after disaggregation [cf. Fig. 2(D)] as a complementary assay.

The higher heat resistance of the disaggregation activity in comparison to the proteolytic activity enabled us to test whether the disaggregation activity itself can be compromised by proteolysis. Wild-type worm PDS was pretreated without or with proteinase K (100 μg/mL) for 1 h at 37°C before inactivation of the proteinase K activity by heating to 80°C for 10 min (conditions that leave the disaggregase intact). The capacity to disassemble ThT-binding Aβ40 fibrils

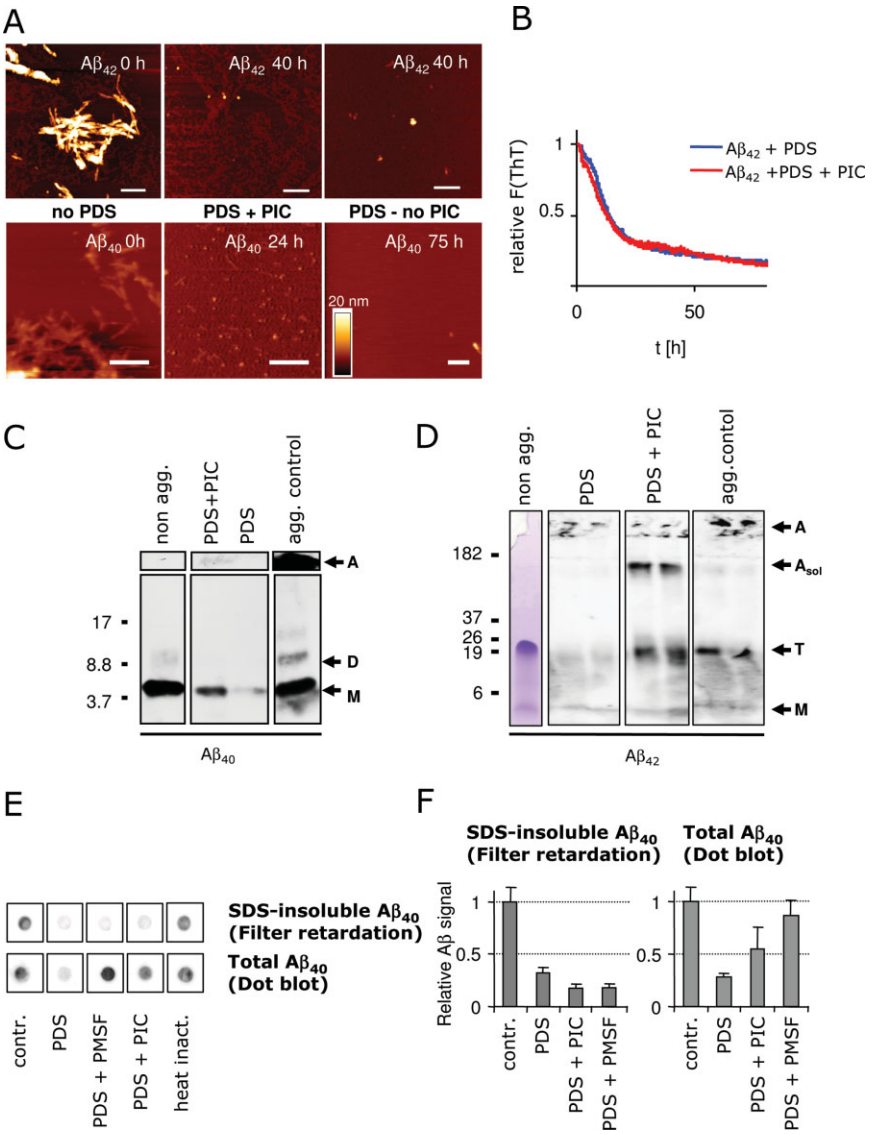

Figure 2. Disaggregation activity is distinct from proteolysis. A: Atomic force microscopy images of fibrillar $A\beta_{42}$ and $A\beta_{40}$ incubated in the presence or absence of *C. elegans* PDS (25 μg/mL) and Roche complete protease inhibitor cocktail (PIC). Scale bars = 200 nm, height scale = 20 nm. Incubation with PDS leads to a loss of readily detectable fibrillar structures both in the presence and absence of PIC. B: Kinetic measurement of Thioflavin T fluorescence of $A\beta_{42}$ incubated for 75 h with PDS in the presence or absence of PIC. C: Western blot of (mAb 6E10) of monomeric $A\beta_{40}$ peptide (non agg.), $A\beta_{40}$ aggregates (agg. control), and the disaggregation products resulting from PDS treatment (25 μg/mL) in the absence or presence of PIC. Arrows indicate apparent monomer (M), dimer (D) and high-MW aggregate (A) bands. D: Coomassie staining reveals monomeric and tetrameric bands of non-aggregated (non agg.) $A\beta_{42}$. Western blot of $A\beta_{42}$ aggregates (agg. control), and the disaggregation products resulting from PDS treatment (25 μg/mL) in the absence or presence of PIC. $A\beta_{42}$ is degraded and proteolyzed after incubation with *C. elegans* PDS for 72 h in the absence of PIC; bands labeled as in C, in addition a soluble aggregate band was observed (A_{sol}). E: Aβ aliquots from disaggregation assays were analyzed by dot blots and filter retardation assays, respectively, after incubation of $A\beta_{40}$ for 72 h to quantify the amounts of total Aβ and SDS-resistant Aβ aggregates. F: Quantification of filter retardation assay and dot blot data. Error bars indicate standard deviations in three independent disaggregation experiments. SDS-resistant, aggregated Aβ is reduced after incubation with *C. elegans* PDS. Total amounts of Aβ peptide remain constant after incubation in the presence of PIC or phenylmethylsulfonylfluoride (PMSF), but decrease in the absence of protease inhibitors.

was greatly reduced in the protease- and heat-treated PDS when compared with PDS that had been heat treated but had not been subjected to proteinase K treatment [Fig. 3(E)], demonstrating that a protein(s) is largely responsible for the disaggregase activity(ies) in *C. elegans*.

Disaggregation is reversible in the absence of proteolysis upon exhaustion of the disaggregase activity

If the disaggregation activity is enabled by a pathway or a specific protein or protein complex that is separable from proteolysis, Aβ monomers released by the

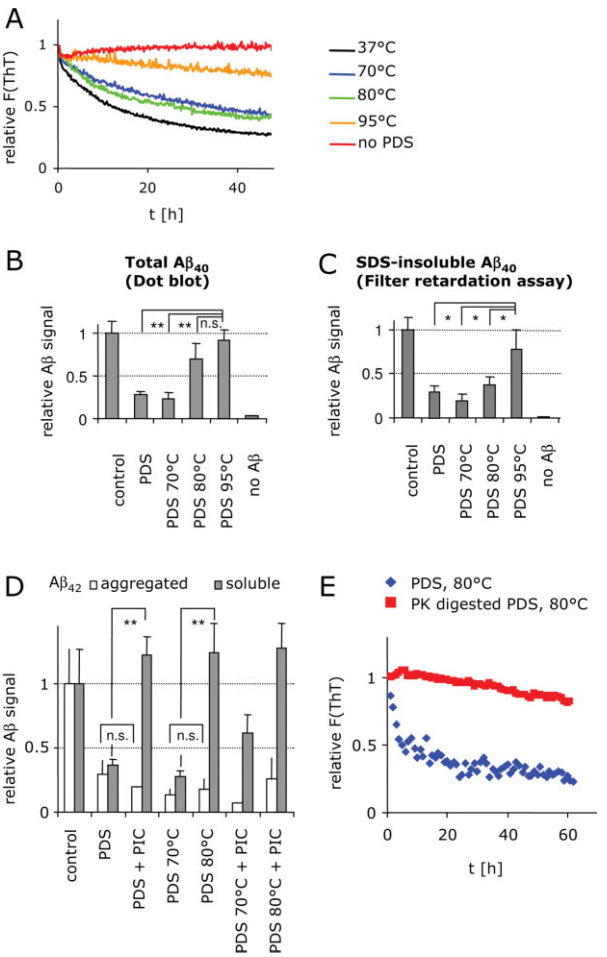

Figure 3. Disaggregation activity is heat resistant A: Heat-treated *C. elegans* PDS (25 μg/mL) incubated with fibrillar $A\beta_{40}$ in the absence of protease inhibitor. PDS was heated to 37, 70, 80 or 95°C for 10 min before incubation with $A\beta_{40}$ fibrils. B: Dot blot quantification of total $A\beta_{40}$ using mAB 6E10 after 72 h incubation. C: $A\beta_{40}$ SDS-resistant aggregate quantification after 72 h incubation (filter retardation, mAB 6E10). Bar graphs show normalized averaged dot blot signals of three independent experiments, error bars indicate standard deviations. Proteolytic activities are inactivated at 70°C, whereas 95°C is needed to inactivate the disaggregation activity D: Fibrillar $A\beta_{42}$ was incubated with heat-treated *C. elegans* PDS as in A in the presence or absence of PIC. Disaggregation products were analyzed by Western blotting as in Fig. 2(D). SDS-insoluble aggregate bands (A) and 20 kDa tetramer bands (T) were analyzed quantitatively. Bar graphs show intensities of aggregate (*white*) and soluble (*gray*) $A\beta_{42}$ peptide bands relative to the amounts of Aβ before incubation (control) from four independent experiments, * denotes $P < 0.05$; ** denotes $P < 0.01$. E: *C. elegans* PDS was pretreated without (blue) or with proteinase K (100 μg/mL) (red) for 1 h at 37°C before inactivation of the proteinase K activity by heating to 80°C for 10 min (conditions that leave the disaggregase intact) and then added to fibrillar $A\beta_{40}$ (15 μ*M*; Aβ monomer).

disaggregase activity could reaggregate when proteases are inhibited, provided that the disaggregase activity is significantly reduced or extinguished. Spontaneous reaggregation of $A\beta_{40}$ after 25 h was indeed observed [Fig. 4(A)] in the presence of the PIC (blue) and PMSF (red). AFM imaging of the $A\beta_{40}$ samples after 75 h of incubation with Aβ worm PDS in the presence of PIC or PMSF confirmed the re-emergence of fibrillar aggregates. Compare Fig. 4(B) with Fig. 2(A), bottom right, $A\beta_{40}$ with PDS in the absence of PIC.

To verify the mass balance and the aggregation state of the Aβ peptide during the disaggregation and reaggregation processes, the amounts of aggregated and monomeric $A\beta_{40}$ peptide were quantified by HPLC analysis. The $A\beta_{40}$ peptide (15 μ*M*) was incubated in PBS at 37°C for 75 h with rotary agitation (20 rpm) to form fibrillar aggregates and then incubated for a further 24 or 75 h in the presence of PDS (1%), either in the presence or absence of PIC. Aliquots of the peptide were ultracentrifuged (200,000 × g, 20 min) at 24 or 75 h, supernatants were removed and pellets were solubilized in HFIP/TFA overnight. Supernatant and pellet fractions were then analyzed by reverse phase HPLC and quantified by UV absorption at 215 nm. Peptide fractions were quantified relative to the initial amount of soluble $A\beta_{40}$ peptide [Fig. 4(C)]. While more than 95% of the Aβ peptide was found in the pellet fraction after aggregation, incubation with PDS for 24 h reduced the quantity of Aβ to ~40% (no PIC). While most of the soluble Aβ was degraded by proteolysis in the absence of PIC, addition of PIC largely prevented proteolysis of soluble Aβ. Interestingly, ~80% of Aβ was again found in the insoluble fraction after prolonged (75 h) incubation with PDS and PIC, consistent with reaggregation.

To further verify that proteolysis prevents reaggregation of $A\beta_{40}$ after incubation with worm PDS, heat-inactivated PDS (5% v/v) was added to freshly monomerized $A\beta_{40}$ (15 μ*M*) and aggregation was monitored by ThT fluorescence [Fig. 4(D)]. The $A\beta_{40}$ peptide aggregated [Fig. 4(D), red lines] in the presence of heat-inactivated PDS (10 min, 95°C) or PDS with added protease inhibitor cocktail [*PIC,* Fig. 4(D), blue lines], on a similar time scale as in the absence of PDS (Supporting information Fig. S1A). In contrast, proteolytically active PDS largely prevented aggregation (green lines). The ThT signal of PDS incubated without $A\beta_{40}$ did not increase with time (orange lines).

Taken together, our results demonstrate that disaggregation and proteolysis are distinct *C. elegans* PDS activities that can be dissociated and monitored separately.

Discussion

The *C. elegans* Aβ disaggregation activity appears to be a primary mechanism for the detoxification of Aβ aggregates in the worm AD model.[22] The disaggregase activity is partially upregulated by activation of the HSF-1 transcription factor, which is negatively regulated by the insulin growth factor-1 receptor signaling pathway that also influences longevity and

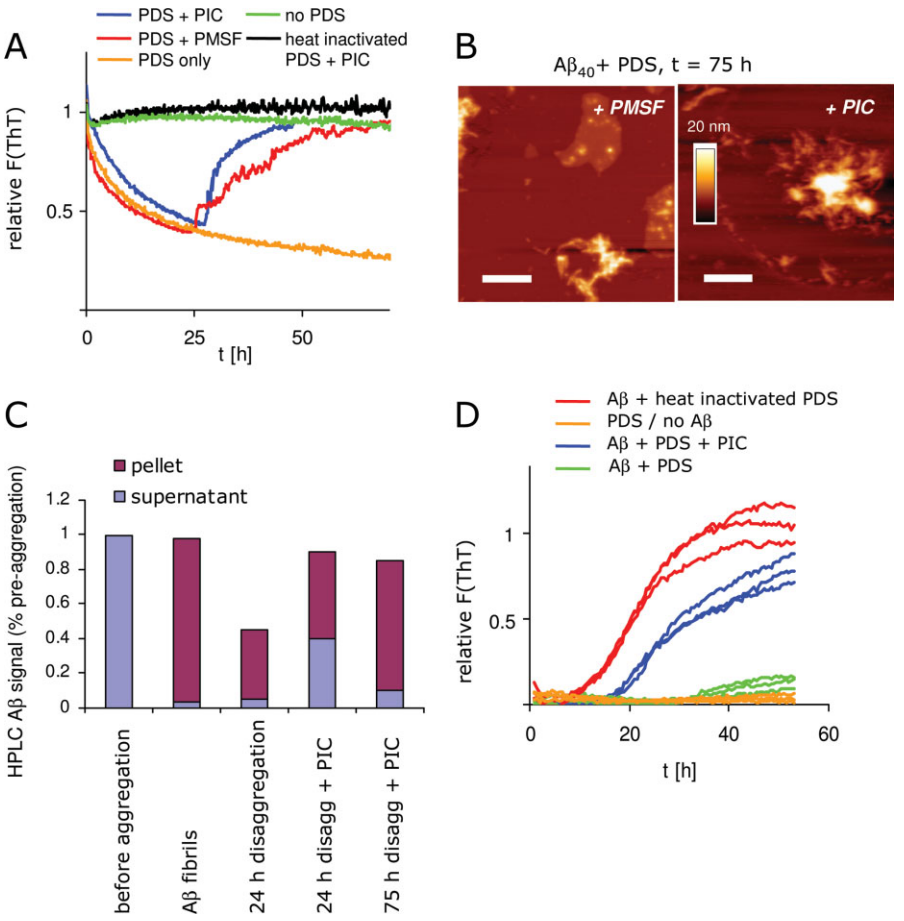

Figure 4. Disaggregation is reversible in the absence of proteolysis. A: *C. elegans* PDS was incubated with $A\beta_{40}$ fibrils for 75 h (as in Fig. 1) in the absence (orange) or presence of PIC (blue) or PMSF (red). Inhibition of proteolysis did not prevent disaggregation, but led to reaggregation of $A\beta_{40}$ upon prolonged incubation. No disaggregation was observed in the presence of heat-inactivated (95°C) PDS in the presence of PIC (green) or in buffer controls (black). B: Atomic force microscopy image of $A\beta_{40}$ fibrils after 75 h incubation with PDS in the presence of PIC or PMSF, showing re-emergence of fibrils. Scale bars = 200 nm, height scale = 20 nm. C: $A\beta_{40}$ peptide (15 μ*M*) was separated into soluble and insoluble fractions by centrifugation at 200,000 × g before and after aggregation and after incubation with PDS (25 μg/mL) in the presence or absence of PIC. Both the pellet and the supernatant were treated with HFIP/TFA to denature $A\beta_{40}$ allowing it to be quantified by HPLC analysis. D: Addition of untreated PDS (5% v/v) to soluble $A\beta_{40}$ (15 μ*M*) [buffer and incubation as in Fig. 1(A)] prevents aggregation of Aβ into ThT-binding aggregates (triplicate samples, green lines), whereas heat-inactivated PDS (95°C, triplicate samples, red lines), and PDS in the presence of PIC (triplicate samples, blue lines) ultimately allowed $A\beta_{40}$ aggregation, apparently after the consumption of the disaggregase activity.

youthfulness. The more detailed characterization of the disaggregase activity outlined herein provides a means to systematically fractionate the cellular components and/or the underlying molecular determinants that disaggregate and degrade Aβ fibrils and perhaps oligomeric aggregates. Herein we have demonstrated that disaggregation and proteolysis are separable cellular activities, both critical for the clearance and detoxification of Aβ aggregates. Both activities may be part of the same macromolecular complex or pathway, yet more experiments are required to identify their origins. The widely available genetic tools and the ease with which gene expression within the nematode *C. elegans* can be manipulated by RNAi enables candidate genes of the Aβ disaggregase activity to be evaluated in this organismal model.

Disaggregation and proteolysis are separate cellular activities

Three unrelated results indicate that disaggregation and proteolysis are separable activities. First, the Roche protease inhibitor cocktail (PIC) and the protease inhibitor PMSF do not affect disaggregation, but largely abolish proteolysis. Second, the disaggregation activity is more resistant to heat inactivation than is the proteolysis activity, as an 80°C pretreatment only moderately slows disaggregation, but largely abolishes proteolysis of Aβ. Third, our data show that spontaneous reaggregation occurs after nearly complete disaggregation when proteolysis is inhibited. Taken together, these results clearly indicate that these two cellular activities are separable, and that the disaggregase activity is protein based, as assessed by the ability

of proteinase K to disable the disaggregase activity. Furthermore, our data suggest that proteolysis of amyloidogenic peptides after disaggregation may be required for the detoxification of amyloid aggregates to prevent their reaggregation into toxic structures.

Candidates to mediate disaggregation

The cellular components or pathway(s) that play a role in the *C. elegans* disaggregation/proteolysis activities are currently unknown. The thermal denaturation resistance of the disaggregase activity is high when compared with the protease activity. Nevertheless, the disaggregase activity can be inactivated by proteolysis, which suggests that it is mediated by a stable protein, protein complex, or pathway, possibly involving membranes or vesicle association. This hypothesis is supported by the finding that detergents compromise the disaggregation activity even at concentrations below those which would denature proteins.

In yeast, Hsp104/ClpB, a AAA ATPase family member, is known to mediate disaggregation[33,34] with a dependence on Hsp70.[35] Owing to the lack of an obvious Hsp104 homolog in mammals, the identity of the disaggregation-mediating protein, protein complex or pathway in mammals remains unknown, and is the subject of ongoing investigations.

The disaggregation assay described herein provides the means to identify the protein(s) and/or pathways responsible for disaggregation and/or proteolysis of Aβ fibrils by analyzing worm homogenate fractionated by chromatographic and related strategies. Using PDS from worms also enables investigation of candidate genes using RNAi approaches that are straightforward to apply in *C. elegans* proteotoxicity models. The disaggregase/proteolysis assay reported herein also enables small molecule screens to be conducted to discover compounds that enhance or inhibit these critical activities. Disaggregase enhancers may be useful for ameliorating aging-associated intracellular Aβ aggregation and proteotoxicity thought to cause neurodegeneration in Alzheimer's disease.

MATERIALS AND METHODS

Materials

Protein concentration was determined using a BCA kit (Pierce #23223). Complete protease inhibitor cocktail (PIC, #1836170) was purchased from Roche (Basel, Switzerland). Synthetic $A\beta_{40}$ and $A\beta_{42}$ peptides were purchased from Synpep (Dublin, CA). Monoclonal anti-Aβ antibodies 4G8 and 6E10 were purchased from Signet (Dedham, MA). All other materials were purchased from Sigma.

C. elegans

CL2006 and control (wt) worms (N2)[21] were obtained from the Caenorhabditis Genetics Center (Minneapolis, MN). The worms were grown at 20°C as previously described.[22]

In vitro *Aβ disaggregation assay*

C. elegans worms grown to day one of adulthood were washed twice with M9 buffer (Sigma) and once more with PBS at room temperature. The worms were then resuspended in 300 μL ice cold PBS, transferred to a tissue grinder (885482, Kontes, Vineland, NJ) and homogenized. Crude homogenates were centrifuged in a desktop microfuge (Eppendorf 5810R, 3000 rpm, 3 min) to prepare post debris supernatants (PDS). PDS were transferred to new tubes and total protein concentrations were measured with a BCA kit (Pierce, Rockford, IL).

A stock solution of monomeric $A\beta_{40}$ peptide (200 μM) was prepared as described.[29] $A\beta_{40}$ peptide (50 μM) was aggregated in phosphate buffer (300 mM NaCl, 50 mM Na-phosphate, pH 7.4) at 37°C in a 1.5 mL reaction tube under constant agitation using a rocking platform (20 cycles/min) (Fig. 1) or an overhead shaker (20 rpm, Figs. 2–4) for 4 days. $A\beta_{40}$ fibrils were sonicated for 30 min in a water bath sonicator (FS60, Fisher Scientific, Pittsburg, PA) and characterized by far UV CD spectroscopy and atomic force microscopy (Fig. S1). $A\beta_{40}$ peptide was then diluted to a final concentration of 15 μM Aβ and 150 mM NaCl in phosphate buffer (50 mM Na-phosphate, pH 7.4) containing ThT (20 μM) and PDS worm homogenate (25 μg/mL) with or without protease inhibitors as indicated. Synthetic $A\beta_{42}$ was pretreated by an analogous procedure, but using a 30 kDa cut-off filter for the second filtration step during monomerization. All final Aβ concentrations were 15 μM unless indicated otherwise.

Three aliquots (100 μL) of each sample were incubated at 37°C in low-binding, 96-well, clear-bottomed plates (Corning). Samples were agitated for 5 s before each reading and ThT fluorescence was measured using a Gemini SpectraMax EM fluorescence plate reader (Molecular Devices, Sunnyvale, CA) every 10 min. Fluorescence backgrounds from PDS and buffer were subtracted from the ThT signal. Fluorescence data were fit to single exponential decay functions with a time constant τ and a linear term allowing for a sloped postdisaggregation baseline: $F(t) = mt + b + A\exp(-t/\tau)$. τ-values are reported as averages +/− standard deviations determined from at least three independent samples. ThT signals were normalized by setting the fluorescence at t = 0 h to one.

Roche complete protease inhibitor cocktail (PIC) was diluted from aqueous stock solutions (25 x) to final concentrations of 1 x dilution.

ATP hydrolysis

To hydrolyze ATP, PDS samples were preincubated for 15 min at 30°C with apyrase (New England Biolabs) at a final concentration of 0.1 or 0.5 U before adding to

the Aβ aggregates. Under these conditions, 0.25 U apyrase were sufficient to completely hydrolyze the ATP present in the PDS as tested in a luciferase assay (data not shown). Aβ aggregates, PIC and azide (0.02%) were added after hydrolysis as indicated.

Filter retardation assays and dot blotting

Equal volumes of denaturation buffer (Tris buffered saline (TBS) pH 8, 4% SDS) were added to Aβ samples (20 μL). Samples were boiled for 5 min and filtered through a cellulose acetate membrane filter (Bio-Rad) using a 96-well vacuum apparatus (Bio-Rad) as described.[5] For dot blots, Aβ samples (20 μL) were mixed with equal volumes of TBS and filtered through a nitrocellulose membrane filter (Bio-Rad) using the same vacuum apparatus.

Western blotting

SDS-PAGE was performed using 16.5% Tris-Tricine buffered acrylamide gels and the peptides were then blotted onto a PVDF membrane. Western blots, dot blots and filter retardation blots were probed using 6E10 (1:2,000) and 4G8 (1:4,000) antibodies and developed using an ECL system. For reprobing, PVDF membranes were stripped by incubation in 300 mM NaOH (5 min, RT), followed by neutralization by several rinses in TBST (10 mM Tris-HCl pH 7.5, 150 mM NaCl, 0.3% Tween-20). Aβ monoclonal antibodies clone 4G8 (#9220) and clone 6E10 (#9320) were purchased from Signet (Dedham, MA), secondary antibodies from Pierce.

Atomic force microscopy

Aliquots (20 μL) were removed from the $A\beta_{40}$ samples and placed on freshly cleaved mica (1 × 1 cm) and mounted onto a metal or glass sample holder. AFM samples were prepared and imaged as described[22] using a Nanoscope III (Veeco, Santa Barbara, CA) or Nanowizard II AFM setup (JPK, Berlin, Germany).

HPLC quantification

Aβ peptide aliquots (100 μL, 15 μM) were centrifuged (200,000 × g 20 min), supernatants were removed and stored at 4°C and pellets were solubilized overnight in 50μL of hexafluoroisopropanol/trifluoroacetic acid (HFIP/TFA 1:1, v/v) after sonicating for 5 min. Water (50 μL) was added to the HFIP samples. Supernatant and pellet fractions were then analyzed by reverse phase HPLC (μRPC C2/C18SC 2.1/10, GE Healthcare) in a water (0.1% TFA)/acetonitrile (0.1% TFA) gradient and quantified by UV absorption at 215 nm. UV signals were normalized to the equivalent amount of soluble $A\beta_{40}$ peptide.

Acknowledgments

The authors thank S. Kostka and G. Grelle for expert technical support.

References

1. Kelly JW (1998) The alternative conformations of amyloidogenic proteins and their multi-step assembly pathways. Curr Opin Struct Biol 8:101–106.
2. Dobson CM (2003) Protein folding and misfolding. Nature 426:884–890.
3. Selkoe DJ (2004) Cell biology of protein misfolding: the examples of Alzheimer's and Parkinson's diseases. Nat Cell Biol 6:1054–1061.
4. Sekijima Y, Wiseman RL, Matteson J, Hammarstrom P, Miller SR, Sawkar AR, Balch WE, Kelly JW (2005) The biological and chemical basis for tissue-selective amyloid disease. Cell 121:73–85.
5. Scherzinger E, Lurz R, Turmaine M, Mangiarini L, Hollenbach B, Hasenbank R, Bates GP, Davies SW, Lehrach H, Wanker EE (1997) Huntingtin-encoded polyglutamine expansions form amyloid-like protein aggregates in vitro and in vivo. Cell 90:549–558.
6. Bates G (2003) Huntingtin aggregation and toxicity in Huntington's disease. Lancet 361:1642–1644.
7. Prusiner SB (1998) The prion diseases. Brain Pathol 8: 499–513.
8. Tanzi RE, Bertram L (2005) Twenty years of the Alzheimer's disease amyloid hypothesis: a genetic perspective. Cell 120:545–555.
9. Balch WE, Morimoto RI, Dillin A, Kelly JW (2008) Adapting proteostasis for disease intervention. Science 319:916–919.
10. Cohen E, Dillin A (2008) The insulin paradox: aging, proteotoxicity and neurodegeneration. Nat Rev Neurosci 9:759–767.
11. Brignull HR, Morley JF, Morimoto RI (2007) The stress of misfolded proteins: *C. elegans* models for neurodegenerative disease and aging. Adv Exp Med Biol 594: 167–189.
12. Morley JF, Brignull HR, Weyers JJ, Morimoto RI (2002) The threshold for polyglutamine-expansion protein aggregation and cellular toxicity is dynamic and influenced by aging in *Caenorhabditis elegans*. Proc Natl Acad Sci USA 99:10417–10422.
13. Dillin A, Crawford DK, Kenyon C (2002) Timing requirements for insulin/IGF-1 signaling in *C. elegans*. Science 298:830–834.
14. Amaducci L, Tesco G (1994) Aging as a major risk for degenerative diseases of the central nervous system. Curr Opin Neurol 7:283–286.
15. Kenyon C (2005) The plasticity of aging: insights from long-lived mutants. Cell 120:449–460.
16. Holzenberger M, Dupont J, Ducos B, Leneuve P, Geloen A, Even PC, Cervera P, Le Bouc Y (2003) IGF-1 receptor regulates lifespan and resistance to oxidative stress in mice. Nature 421:182–187.
17. Suh Y, Atzmon G, Cho MO, Hwang D, Liu B, Leahy DJ, Barzilai N, Cohen P (2008) Functionally significant insulin-like growth factor I receptor mutations in centenarians. Proc Natl Acad Sci USA 105:3438–3442.
18. Willcox BJ, Donlon TA, He Q, Chen R, Grove JS, Yano K, Masaki KH, Willcox DC, Rodriguez B, Curb JD (2008) FOXO3A genotype is strongly associated with human longevity. Proc Natl Acad Sci USA 105:13987–13992.
19. Hsu AL, Murphy CT, Kenyon C (2003) Regulation of aging and age-related disease by DAF-16 and heat-shock factor. Science 300:1142–1145.
20. Morley JF, Morimoto RI (2004) Regulation of longevity in *Caenorhabditis elegans* by heat shock factor and molecular chaperones. Mol Biol Cell 15:657–664.
21. Link CD (1995) Expression of human beta-amyloid peptide in transgenic *Caenorhabditis elegans*. Proc Natl Acad Sci USA 92:9368–9372.

22. Cohen E, Bieschke J, Perciavalle RM, Kelly JW, Dillin A (2006) Opposing activities protect against age-onset proteotoxicity. Science 313:1604–1610.
23. Chaudhuri TK, Paul S (2006) Protein-misfolding diseases and chaperone-based therapeutic approaches. FEBS J 273:1331–1349.
24. Shorter J, Lindquist S (2004) Hsp104 catalyzes formation and elimination of self-replicating Sup35 prion conformers. Science 304:1793–1797.
25. Solomon B, Koppel R, Frankel D, Hanan-Aharon E (1997) Disaggregation of Alzheimer beta-amyloid by site-directed mAb. Proc Natl Acad Sci USA 94: 4109–4112.
26. Schenk D, Barbour R, Dunn W, Gordon G, Grajeda H, Guido T, Hu K, Huang J, Johnson-Wood K, Khan K, Kholodenko D, Lee M, Liao Z, Lieberburg I, Motter R, Mutter L, Soriano F, Shopp G, Vasquez N, Vandevert C, Walker S, Wogulis M, Yednock T, Games D, Seubert P (1999) Immunization with amyloid-beta attenuates Alzheimer-disease-like pathology in the PDAPP mouse. Nature 400:173–177.
27. Leissring MA, Farris W, Chang AY, Walsh DM, Wu X, Sun X, Frosch MP, Selkoe DJ (2003) Enhanced proteolysis of beta-amyloid in APP transgenic mice prevents plaque formation, secondary pathology, and premature death. Neuron 40:1087–1093.
28. Powers ET, Powers DL (2006) The kinetics of nucleated polymerizations at high concentrations: amyloid fibril formation near and above the "supercritical concentration". Biophys J 91:122–132.
29. Bieschke J, Zhang Q, Powers ET, Lerner RA, Kelly JW (2005) Oxidative metabolites accelerate Alzheimer's amyloidogenesis by a two-step mechanism, eliminating the requirement for nucleation. Biochemistry 44:4977–4983.
30. Levine H (1999) Quantification of beta-sheet amyloid fibril structures with thioflavin T. Methods Enzymol 309: 274–284.
31. Krebs MR, Bromley EH, Donald AM (2005) The binding of thioflavin-T to amyloid fibrils: localisation and implications. J Struct Biol 149:30–37.
32. Klement K, Wieligmann K, Meinhardt J, Hortschansky P, Richter W, Fandrich M (2007) Effect of different salt ions on the propensity of aggregation and on the structure of Alzheimer's abeta(1–40) amyloid fibrils. J Mol Biol 373:1321–1333.
33. Shorter J, Lindquist S (2006) Destruction or potentiation of different prions catalyzed by similar Hsp104 remodeling activities. Mol Cell 23:425–438.
34. Parsell DA, Kowal AS, Singer MA, Lindquist S (1994) Protein disaggregation mediated by heat-shock protein Hsp104. Nature 372:475–478.
35. Glover JR, Lindquist S (1998) Hsp104, Hsp70, and Hsp40: a novel chaperone system that rescues previously aggregated proteins. Cell 94:73–82.